

## Structural, Morphological, and Optical Properties of Zinc Oxide Nanorods for LPG sensor

Ali J. Mohammed

Jalal J. Hassan

S J Kasim

M. A. Mahdi

*Department of Physics Science, University of Basrah*

ali.jasim1993@yahoo.com

**Abstract:**

In this research, zinc oxide nanorods were prepared by chemical bath deposition method (CBD) through using raw materials on the glass substrate. The crystalline structure, surface morphology, elemental composition and optical properties of ZnO were studied by X-ray diffraction pattern (XRD), field emission scanning electron microscopy (FESEM), energy dispersive spectrometers (energy-dispersive X-ray spectroscopy EDXS), and UV-vis spectrophotometer, respectively. The sensing properties of the ZnO nanorod arrays were determined for different flows and temperatures. The results indicate that the ZnO nanorods have good sensitivity and stability when compared with other traditional ZnO films.

**Keywords:** Zinc Oxide (ZnO); Nanorod arrays; Chemical bath deposition (CBD); LPG sensor.

### الخصائص التركيبية والسطحية والبصرية لقضبان الخارصين النانوية لتحسس غاز البترول المسال

علي جاسم محمد، جلال جبار حسن، ستار جبار قاسم، مازن عوني مهدي

قسم علوم الفيزياء جامعة البصرة

**الخلاصة:**

في هذا البحث، تم تحضير قضبان اوكسيد الخارصين النانوية بطريقة الحمام الكيميائي باستخدام المواد الخام على قواعد الزجاج. تم دراسة الخصائص التركيبية والسطحية والتكوينية والبصرية لقضبان اوكسيد الخارصين النانوية عن طريق حيود الاشعة السينية والمجهر الالكتروني الماسح الضوئي و طيف الامتصاصية. خصائص الاستشعار لقضبان اوكسيد الخارصين النانوية تم تحديدها لعدد مختلف من تدفقات الغاز وكذلك لدرجات حرارة مختلفة. النتائج التي تم الحصول عليها من خلال قضبان اوكسيد الخارصين النانوية تشير الى ان هناك حساسية جيدة واستقرارية عالية مقارنة مع الاغشية الرقيقة التقليدية لاوكسيد الخارصين.

**الكلمات المفتاحية:** أوكسيد الخارصين، مصفوفة القضبان، الحمام الكيميائي، حساس لغاز البترول المسال(غاز الطبخ).

**1. Introduction**

The improvement in the semiconductor metal oxides properties make them valuable for more application in various fields[1]. Direct wide band gab (~3.37 eV)[2] and a large free-exciton binding energy of about (~60 meV)[3, 4]

make ZnO as promising material in excitonic emissions and lasing applications above room temperature compared with other materials. In addition, ZnO is usually an n-type semiconductor because of the presence of oxygen vacancy in ZnO and it acts as electron donor[5].

On the other hand, ZnO has been synthesized in various nanostructures such as nanowires [6], nanobelts, nanotubes[7], and nanorods[6], etc. These different nanostructures make ZnO as the best option for various applications especially in solar cell, and gas sensor due to the high ratio of the surface to volume.

Recently, several studies have been conducted to improve the performance of ZnO sensors in order to enhance sensitivity and response time and to decrease the working temperature [8]. Many synthesis methods have been employed to prepare ZnO nanorods[9], such as vapor-liquid-solid [10], metal organic chemical vapor deposition [11], laser ablation-catalytic growth [12], pulsed laser deposition [13], hydrothermal [14], and chemical bath deposition (CBD) method [15, 16]. Recently, chemical bath deposition (CBD) method has been widely adopted because of it does not need vacuum system or high temperature. Moreover, CBD method is a simple and economical approach for the growth nucleation of zinc oxide (ZnO) and it can achieve many different morphologies and different properties for ZnO nanostructures.

In this paper, ZnO nanorods arrays were fabricated with aligned uniform diameter on glass substrates using a chemical bath deposition method at normal atmospheric pressure without any metal catalyst. The ZnO nanorods sensor shows high sensitivity, stability and good response and recovery time. The results indicate that the ZnO nanorods are potential options for improving sensitivity and stability of sensors. Many steps were followed to formulate the ZnO nanorods where the first started with using the sol-gel method to synthesize ZnO seed layers.

## 2. Experiment Details

### 2.1 Materials and Sol Formation

For this research, all chemical reagents were purchased commercially and utilized without further purification. ZnO nanostructures were synthesized from the cost-effective zinc acetate dehydrate  $(C_2H_3O_2)_2 Zn \cdot 2H_2O$ . To start with 1.5 g of zinc acetate was dissolved in 50 ml of ethanol by stirring for 1 h at room temperature in order to obtain a homogenous solution. Then 4ml of Diethanolamine was added to the obtained homogeneous solution and then mixed by a magnetic stirrer for 15 minutes at maintained room temperature.

### 2.2 Seed Layer Preparation

The seed layers were coated on a clean glass substrate by means of sol-gel method, which started by spin-coating process. Seed sol is used to synthesize the thin seed layers. The glass substrates were cleaned with HCl, Acetone, ethanol and deionized water by a utilized ultrasonic instrument and dried at room temperature. The coating process was done with rotation around 2700 rpm within 60 sec for each once. After coating each spin, all the films were dried at 200°C for 2 minutes. Then, six layers were deposited on each substrate to obtain the desired thickness. Finally, all the films were annealed through using a hot plate at 350°C for 2 h to convert (ZnAc) to ZnO nucleation arrays. Finally, the ZnO growth process was conducted by using the chemical bath deposition.

### 2.3 Growth of ZnO nanorods

The chemical bath deposition method CBD was employed to synthesize ZnO nanorods after deposition seed layer of ZnO step, as shown in Figure 1. The precursor solutions were combined as 1.5g Zinc nitrate hexahydrate  $(Zn(NO_3)_2 \cdot 6H_2O)$ ,

99.9% purity) and 0.8 g hexamethylenetetramine (HMT, C<sub>6</sub>H<sub>12</sub>N<sub>4</sub>, 99.9% purity) that individually dissolved into 20 ml distilled water at room temperature with magnetic stirrer for 30 minutes by utilized quartz beakers. The seeded substrates were placed vertically in a bath at 90 °C into the third quartz beaker containing 50ml deionized water on the hot plate for 2h. Then, the growth process started through mixing the two solutions by dipping in the third beaker. This growth process continued for 2 hours. Figure 1 shows the steps of the fabrication process of ZnO nanorod arrays.

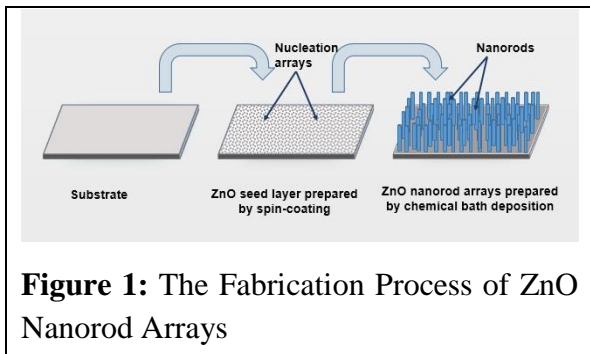


**Figure 1:** The Fabrication Process of ZnO Nanorod Arrays

### 2.4 Fabrication of Electronic Gas Testing System

Nowadays, the most important thing to start to study gas sensor application requires how can build testing system able to test the samples without any danger on researchers. Therefore, it is very necessary to construct an electronic system that tests the samples with significant advantages, such as high accuracy and low cost. Electronic sensor system was constructed in the unit of nanotechnology laboratory at physics department/ college of Science at the University of Basrah to measure the sensitivity of ZnO nanorod arrays samples for various types of gas, such as LPG and CO<sub>2</sub> gas.

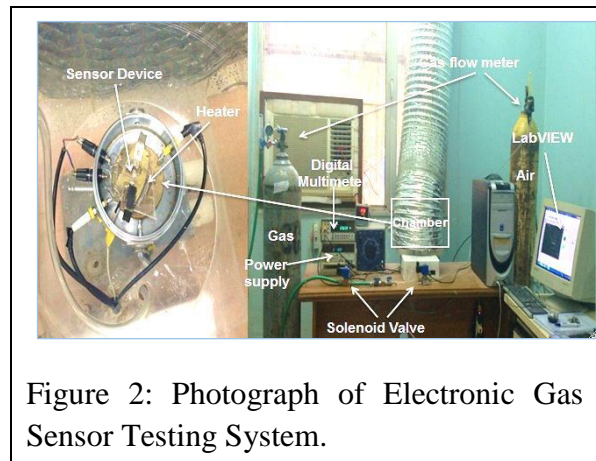


**Figure 2:** Photograph of Electronic Gas Sensor Testing System.

The sensor system includes: pressure regulators, sensing chamber, silica tube air dryer, cylinder gas, heated sample holder, mass flow controller, and required electronics (solenoid valve). These elements are used to control the gas flow and time inside the test chamber. Figure 2 depicts the elements of the electronic gas sensor testing system that was set up in the lab.

The flow rate of testing gas was varied in accordance with the required gas flow. The sensor response was measured by the following relation below (1)[17], as LPG belongs to the category of reducing gasses:

$$S = \frac{I_g - I_a}{I_a} \times 100 = \frac{\Delta I}{I_a} \times 100 \quad (1)$$

Where (S) is the sensitivity of ZnO nanorod arrays sensor,  $I_a$  is the value of the current in the presence of air and  $I_g$  is the value of the current after exposure to the gas. The sensor signal acquisition was automated and performed through the dedicated Lab-VIEW software code developed in-laboratory. The Lab-VIEW software in coordination with GPIB/USB interface enables to reception and transfer data between the computer and digit multimeter.

The current–time measurements were performed at various working

temperature using digit multimeter (FLUKE 8808 used for current measurement) and a voltage current source.

### 2.5 Characterization Methods

The nanomaterial was investigated as-synthesized material by X-ray diffraction (XRD) using a X'pert Modular Powder Diffractometer equipped with CuK $\alpha$  wavelength of radiation ( $\lambda = 1.54056 \text{ \AA}$ ). The morphological details of nanostructure were characterized by field-emission scanning electron microscopy (FESEM, Zeiss Supra, Germany). The elemental composition of ZnO nanorods was studied by utilization energy-dispersive spectrometers (energy-dispersive X-ray spectroscopy EDXS). Furthermore, the optical properties of ZnO nanorods were reveal by using UV-vis spectrophotometer. Additionally, the electrical properties of chemically deposited ZnO nanorod arrays and their gas sensing characteristics to LPG are discussed.

### 3. Result and Discussion:

The X-Ray diffraction pattern of the nanostructure is studied with the diffraction angle  $20^\circ - 70^\circ$ . All The diffraction peaks in the pattern are matching with the ZnO hexagonal phase of JCPDF No.36-1451 and the data are in agreement with JCPDS card for ZnO. Figure 3: shows the XRD pattern of vertically aligned ZnO nanorods grown on glass substrate. There are no other characteristic impurities peaks were presented which also confirm that the product obtained is in pure phase. The intensity of the peak assigned to the (0 0 2) plane of hexagonal wurtzite type ZnO was markedly large and the diffraction peaks of other crystal planes almost disappeared or were very weak, the (0 0 2) plane is

strongly oriented perpendicularly to the substrate surface. Thus, the columnar rods composing the films are formed through elongation along the c-axis[18]. The average crystalline size (D) of ZnO nanorods is estimate by the following Eq (2) [19, 20].

$$D = \frac{k \lambda}{\beta \cos \theta} \tag{2}$$

Where  $\lambda$  is the X-ray wavelength of  $1.54 \text{ \AA}$ ,  $\beta$  is the full width at half maximum (FWHM) of the XRD,  $k$  is a numerical constant for which Scherrer obtained the value  $2(\ln 2 / \pi)^{0.5} = 0.9394$  and  $\theta$  is the Bragg diffraction angle can be represented by d-spacing (d) between the atomic planes (002), calculated by Bragg's law (3)[2].

$$n \lambda = 2d_{hkl} \sin \theta_{hkl} \tag{3}$$

Where n is a positive integer. In addition, the lattice constants (a, and c) of ZnO nanorods grown on glass substrate were calculated by using the following Eq(4)[2].

$$\frac{1}{d_{hkl}^2} = \frac{4}{3} \left( \frac{h^2 + hk + k^2}{a^2} \right) + \frac{l^2}{c^2} \tag{4}$$

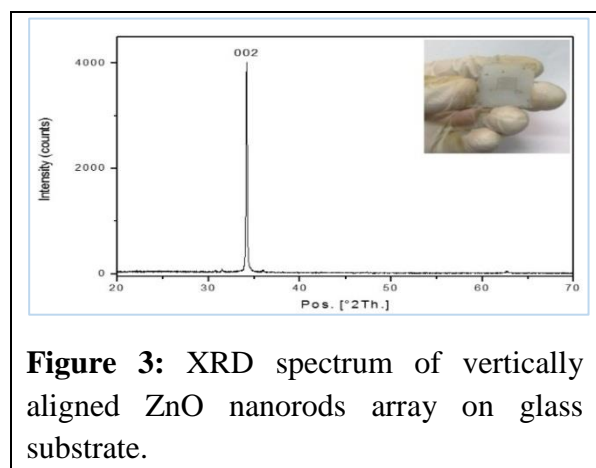


**Figure 3:** XRD spectrum of vertically aligned ZnO nanorods array on glass substrate.

The Lattice parameters, grain size, and c/a ratio of ZnO nanorods grown on glass substrate can be seen in Table 1.

**Table 1.** Lattice parameters, grain size, and c/a ratio of ZnO nanorods grown on glass substrate calculated from XRD data

Fuel	Unit cell Parameters (nm)		Av. crystalline size (nm)	c/a ratio
	A	C		
HMTA	0.3214611	0.524946	60.27904	1.633

Figure. 4(a), and (b) show micrographic (FESEM) of ZnO nanostructure grown onto glass substrate at two different magnifications (140 KX, and 18 KX). The images show the vertically aligned ZnO nanorods along the c-axis with high distribution density was grown on the substrate surface. The nanorods have hexagonal shapes with uniform diameter. In addition, Figure. 4(c) illustrates the diameters distribution of the nanorods on the surface of glass substrate in the range of 80-300 nm.

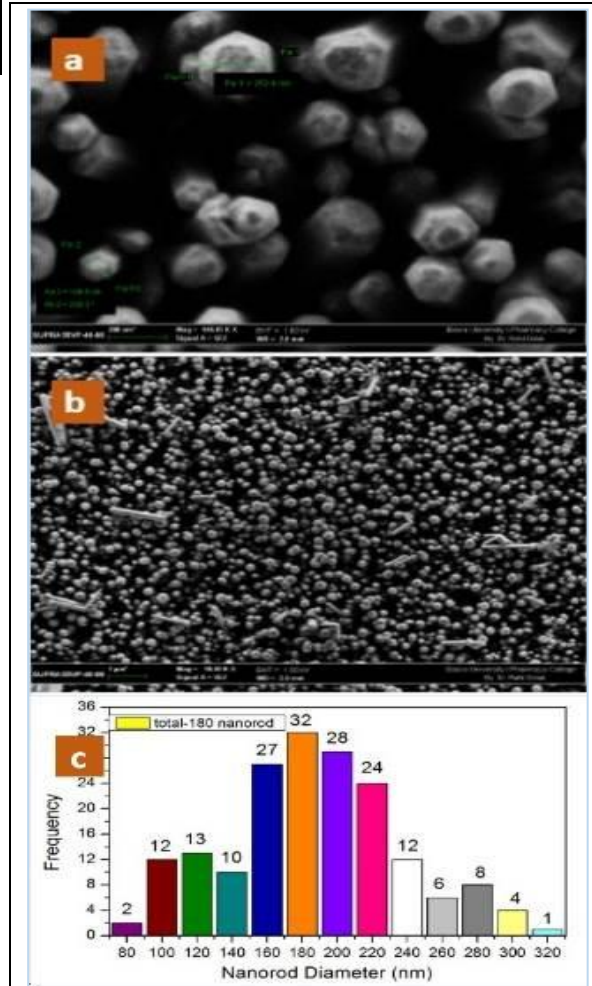
Figure 5: represents The (EDX) spectrum analysis of the ZnO nanorod arrays sample shows only Zn and O signal peaks. The elemental composition of ZnO nanorods approximate atomic ratio of zinc and oxides is found to be 42.11: 57.89.

Figure 6 shows the I-V characteristics of ZnO nanorod arrays at room temperature in presence of air .It shows a symmetrical behavior indicating ohmic nature of aluminum contacts. It was taken after annealing the ZnO nanorods at 350°C.

Figure 7 shows UV-V absorption of ZnO Nanorod arrays grown on glass substrate. The adsorption edge of ZnO Nanorod arrays is about 400 nm that related to optical band gap of ZnO.This adsorption spectrum describe the high transmission of ZnO Nanorod at energies lower than energy gap of ZnO nanorods.

The optical energy gap can be estimated by calculating the optical absorption coefficient ( $\alpha$ ), which depends on the absorbance and film thickness of the sample as given in the following equation.

$$\alpha = 2.303A/t \tag{5}$$



**Figure 4:** FESEM images of vertically aligned ZnO nanorods grown onto a glass substrate, (a) is a magnified image at (140 KX), (b) is a magnified image of the same (18 KX), and (c) ZnO nanorods diameter distributions.

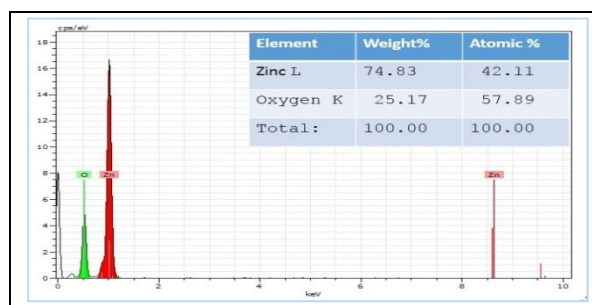


**Figure 5:** The energy-dispersive X-ray spectroscopy (EDAX) Analysis of the ZnO Nanorod arrays.

Where ( $\alpha$ ) is the optical absorption coefficient, which can be calculated from absorbance and thickness of the sample using: ( $\alpha=2.303A/t$ ); and ( $h\nu$ ) can be calculated from wavelength using: ( $h\nu = 1240/\lambda$ ). The energy band gap ( $E_g$ ) was calculated using figure 6 (b). The value of the optical band energy was found to be 3.2 eV.

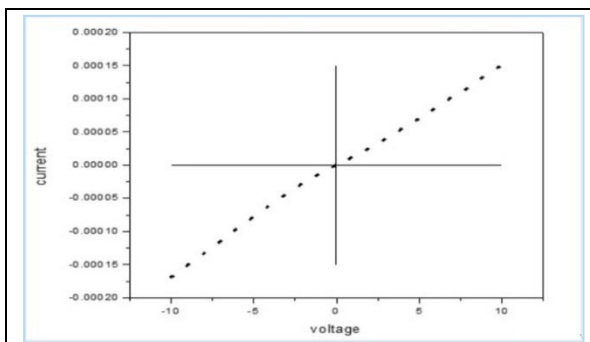


**Figure 6:** Room Temperature I-V Curve of Al Grid Showed Ohmic Behavior between Grid and Semiconductor

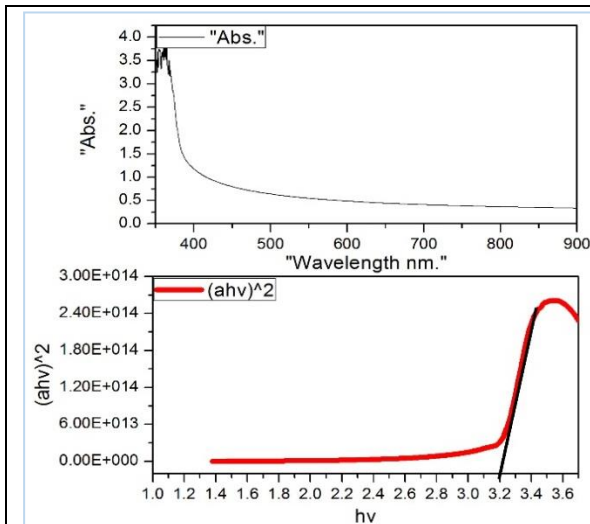
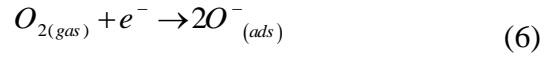
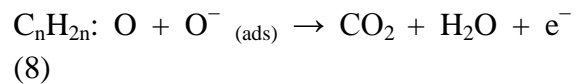
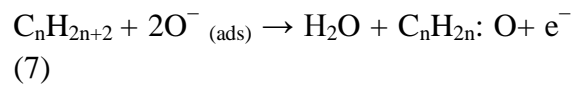


**Figure 7:** (a) UV-Visible Absorption Spectra of ZnO Nanorod Arrays (b) Plot of  $(ah\nu)^2$  versus  $(h\nu)$  for determination of band gap of ZnO nanorods.

The exposed surface of ZnO nanorods adsorbs the oxygen molecules from the ambient air, which import conduction electrons to form adsorbed oxygen ions on the surface of the rods to formation depletion layer, given as[21].



When the sensor is exposed to the gas molecules, the molecules of gas interact with the adsorbed oxygen ions present on the surface of the sensor as shown in Eq.(6) and released the trapped electrons back to the conduction band. This leads to an increased carrier concentration of ZnO and increasing the current of the sensor. The overall reaction of LPG molecules with the adsorbed oxygen species can be explained based on the following reactions[22]:



Where,  $C_nH_{2n+2}$  represents the hydrocarbons of LPG, propane ( $C_3H_8$ ), and butane ( $C_4H_{10}$ ).

Figure 8: shows the sensitivity of ZnO nanorods at operating temperature 250°C, with three different flows for the same temperature. Where the red, green, and black line represents the sensitivity at the 1, 2, and 3 liters/minute flow. From the figure it clear the ZnO has maximum sensitivity at working temperature (250°C) reached (823%) of 3 liter/minute flow gas at response and recovery time of 135 s and 21 s, respectively. The response is define as time require to reach 90% of saturation current upon exposure to test LPG and recovery time is define as time required for

recovering 90% of original current of the sensor.

Table 2 shows that the LPG sensitivity of the sensor in the present work (this work) is 823%. Which is much more high as compared to 3% recorded in [23], 8.02 recorded in [24] and other reported in [5], [25], and [26]. the larger sensitivity that has achieved in the present work may be because of the nanostructure has the Large surface area to volume ratio due to the nanorods have small diameters i.e. the more atoms ready to interaction with the gas molecules, as well as small diameters means that the depletion layer increase

compares with the conductive channel. On the other hand, Figure 9: shows the sensitivity as a function of operating temperature for ZnO nanorods obtained at different temperatures, under the exposure of 3lit/min of LPG. This Figure reveals that each operating temperature has different sensitivity and sensitivity increase with high operating temperatures. To this, it is observed from figure 9 that at operating temperature 275°C exhibits the highest sensitivity (1112%) compared with the other temperatures due to ZnO nanorods requires the relatively higher working temperature to adsorb the oxygen atoms to formation the depletion layer.

Table 2. Comparison of LPG sensing properties of previously recorded with the sensor in the present work

Material	Temperature (°C)	Concentration	Response time	Recovery time	Sensitivity (S)	Ref.
ZnO nanorods	332	200 ppm	10 sec	30 sec	3%	[23]
ZnO thick films	350	100 ppm	.....	.....	8.02	[24]
ZnO nanorods	300	2600 ppm	.....	.....	37%	[5]
ZnSnO3: ZnO nanowire	room temperature	4000 ppm	.....	.....	67.52%	[25]
ZnO nanostructure	450	0.7 %	.....	.....	160	[26]
ZnO nanorods	250	3 lit/min	135 sec	21 sec	823%	This work.

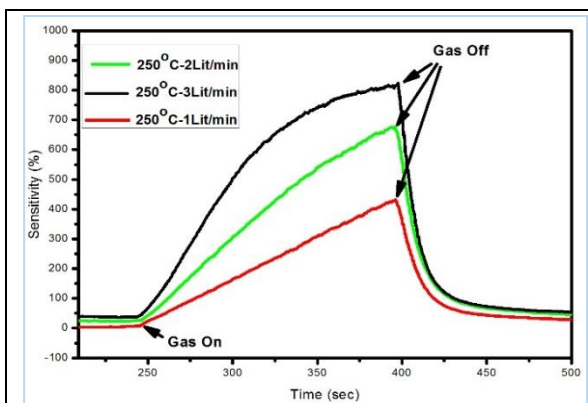


Figure 8: sensitivity of ZnO nanorods to LPG at three different flow at 250°C.

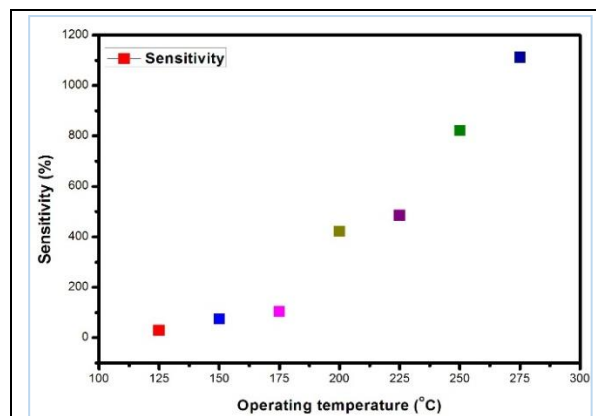


Figure 9: LPG response as a function of operating temperature for ZnO nanorods obtained at different bath temperatures upon exposure to 3Lit/min flow of LPG.

#### 4. Conclusions

ZnO nanorods sample could be prepared on glass substrate using inexpensive and simple chemical bath deposition technique. The ZnO nanorods sensor in the present work showed remarkable enhancement of LPG response over the other traditional ZnO films and other oxide thick films. In addition, The ZnO nanorods has a high sensitivity to LPG and as well as exhibits rapid response and recovery time which is one of the main features of this sensor.

#### 5. Acknowledgments

The authors gratefully acknowledge support from a university of Basra.

#### 6. Reference

- [1] Priya, S.M., A. Geetha, and K. Ramamurthi, Structural, morphological and optical properties of tin oxide nanoparticles synthesized by sol–gel method adding hydrochloric acid. *Journal of Sol-Gel Science and Technology*, 2016. 78(2): p. 365-372.
- [2] Hsu, J.-C. and Y.-S. Chiang, Influence of oxygen on zinc oxide films fabricated by ion-beam sputter deposition. *ISRN Materials science*, 2013. 2013.
- [3] Janotti, A. and C.G. Van de Walle, Fundamentals of zinc oxide as a semiconductor. *Reports on progress in physics*, 2009. 72(12): p. 126501.
- [4] Hassan, J., et al., Microwave assisted chemical bath deposition of vertically aligned ZnO nanorods on a variety of substrates seeded by PVA–Zn (OH) 2 nanocomposites. *Applied Surface Science*, 2012. 258(10): p. 4467-4472.
- [5] Gurav, K., P. Deshmukh, and C. Lokhande, LPG sensing properties of Pd-sensitized vertically aligned ZnO nanorods. *Sensors and Actuators B: Chemical*, 2011. 151(2): p. 365-369.
- [6] Huang, M.H., et al., Catalytic growth of zinc oxide nanowires by vapor transport. *Advanced Materials*, 2001. 13(2): p. 113-116.
- [7] Sun, Y., et al., Synthesis of aligned arrays of ultrathin ZnO nanotubes on a Si wafer coated with a thin ZnO film. *Advanced materials*, 2005. 17(20): p. 2477-2481.
- [8] Park, S.-H., et al., Zinc oxide thin film doped with Al<sub>2</sub>O<sub>3</sub>, TiO<sub>2</sub> and V<sub>2</sub>O<sub>5</sub> as sensitive sensor for trimethylamine gas. *Sensors and Actuators B: Chemical*, 1998. 46(2): p. 75-79.
- [9] Hassan, J., et al., High sensitivity and fast response and recovery times in a ZnO nanorod array/p-Si self-powered ultraviolet detector. *Applied Physics Letters*, 2012. 101(26): p. 261108.
- [10] Klimovskaya, A., I. Ostrovskii, and A. Ostrovskaya, Influence of growth conditions on morphology, composition, and electrical properties of n- Si wires. *physica status solidi (a)*, 1996. 153(2): p. 465-472.
- [11] Yazawa, M., et al., Effect of one monolayer of surface gold atoms on the epitaxial growth of InAs nanowhiskers. *Applied Physics Letters*, 1992. 61(17): p. 2051-2053.
- [12] Duan, X. and C.M. Lieber, Laser-assisted catalytic growth of single crystal GaN nanowires. *Journal of the American Chemical Society*, 2000. 122(1): p. 188-189.

- [13] Guo, X.-L., et al., Fabrication and optoelectronic properties of a transparent ZnO homostructural light-emitting diode. *Japanese Journal of Applied Physics*, 2001. 40(3A): p. L177.
- [14] Wu, W., et al., Epitaxy of vertical ZnO nanorod arrays on highly (001)-oriented ZnO seed monolayer by a hydrothermal route. *Crystal Growth and Design*, 2008. 8(11): p. 4014-4020.
- [15] Tian, Z.R., et al., Complex and oriented ZnO nanostructures. *Nature materials*, 2003. 2(12): p. 821-826.
- [16] Xu, S. and Z.L. Wang, One-dimensional ZnO nanostructures: solution growth and functional properties. *Nano Research*, 2011. 4(11): p. 1013-1098.
- [17] Dhawale, D., et al., Room temperature liquefied petroleum gas (LPG) sensor. *Sensors and Actuators B: Chemical*, 2010. 147(2): p. 488-494.
- [18] Yamabi, S. and H. Imai, Growth conditions for wurtzite zinc oxide films in aqueous solutions. *Journal of materials chemistry*, 2002. 12(12): p. 3773-3778.
- [19] D'Agostino, A.T., Determination of thin metal film thickness by x-ray diffractometry using the Scherrer equation, atomic absorption analysis and transmission/reflection visible spectroscopy. *Analytica Chimica Acta*, 1992. 262(2): p. 269-275.
- [20] Nakate, U., et al., Au sensitized ZnO nanorods for enhanced liquefied petroleum gas sensing properties. *Applied Surface Science*, 2016. 371: p. 224-230.
- [21] Gurav, K., et al., Morphology evolution of ZnO thin films from aqueous solutions and their application to liquefied petroleum gas (LPG) sensor. *Journal of Alloys and Compounds*, 2012. 525: p. 1-7.
- [22] Sivapunniam, A., et al., High-performance liquefied petroleum gas sensing based on nanostructures of zinc oxide and zinc stannate. *Sensors and Actuators B: Chemical*, 2011. 157(1): p. 232-239.
- [23] Jiaqiang, X., et al., Hydrothermal synthesis and gas sensing characters of ZnO nanorods. *Sensors and Actuators B: Chemical*, 2006. 113(1): p. 526-531.
- [24] Patil, D. and L. Patil, Cr<sub>2</sub>O<sub>3</sub>-modified ZnO thick film resistors as LPG sensors. *Talanta*, 2009. 77(4): p. 1409-1414.
- [25] Fu, Y., et al., Detecting liquefied petroleum gas (LPG) at room temperature using ZnSnO<sub>3</sub>/ZnO nanowire piezo-nanogenerator as self-powered gas sensor. *ACS applied materials & interfaces*, 2015. 7(19): p. 10482-10490.
- [26] Latyshev, V., et al., Nanostructured ZnO films for potential use in LPG gas sensors. *Solid State Sciences*, 2017. 67: p. 109-113.